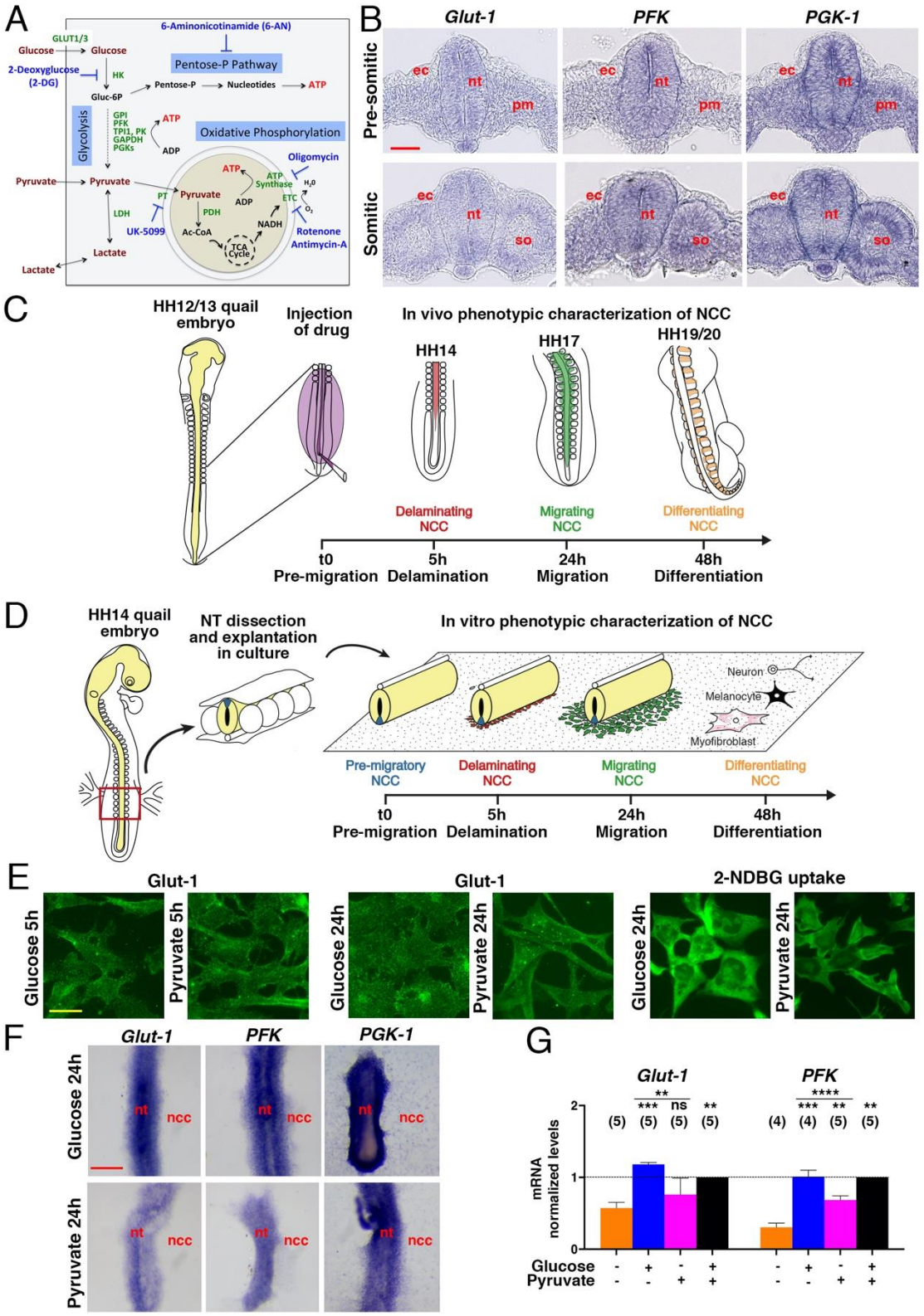

Supplementary Figure 1: Nekooie-Marnany et al.

Fig. S1, related to Fig.1.

(A) Representation of the main pathways of glucose and pyruvate metabolism indicating the specific targets of inhibitors of glycolysis (2-DG), ATP synthase (oligomycin), complex I-III of the electron transport chain (Rot.-AA), mitochondrial pyruvate transporter (UK-5099), and PPP (6-AN) used in this study. (B) Cross sections through the unsegmented paraxial mesoderm (pm) (upper panels) and the last somites (so) (lower panels) of embryos hybridized with probes for *Glut-1*, *PFK* and *PGK-1* mRNAs. The corresponding magnification views of the sections are shown in Fig. 1B. (C, D) Schematic representation of the procedure for *in-ovo* injection of quail embryos and *in vitro* culture of trunk NT explants, respectively, with indication of the timing of NCC development from pre-migration stage to early differentiation. (E) Left: Immunofluorescence staining for Glut-1 transporter on migrating NCCs cultured in glucose or pyruvate medium for 5 h and 24 h. Right: Fluorescent 2-NDBG uptake performed on migrating NCCs in glucose or pyruvate medium after 24-h culture. (F) ISH for *Glut-1*, *PFK*, and *PGK-1* mRNAs on 24 h-NT explants cultured in glucose or pyruvate. (G) Normalized levels. of *Glut-1* and *PFK* in NT explants at 24 h in indicated nutrient conditions measured by qRT-PCR. Measurements were done in triplicates per condition and gene, analyzed using unpaired t-test two-tailed relative to the conditions without glucose and pyruvate and that with both glucose and pyruvate, and presented as mean ± s.e.m. (n) indicate the number of experiments. Data were collected from at least three independent experiments. Images in B, E, and F are representative of these independent experiments. ** $P<0.01$, *** $P<0.001$, **** $P<0.0001$; ns, not statistically significant, $P>0.05$. Scale bars in B and F, 100 µm, and in E, 10 µm. ec, ectoderm; pm, unsegmented paraxial mesoderm; nt, neural tube; so, somite.

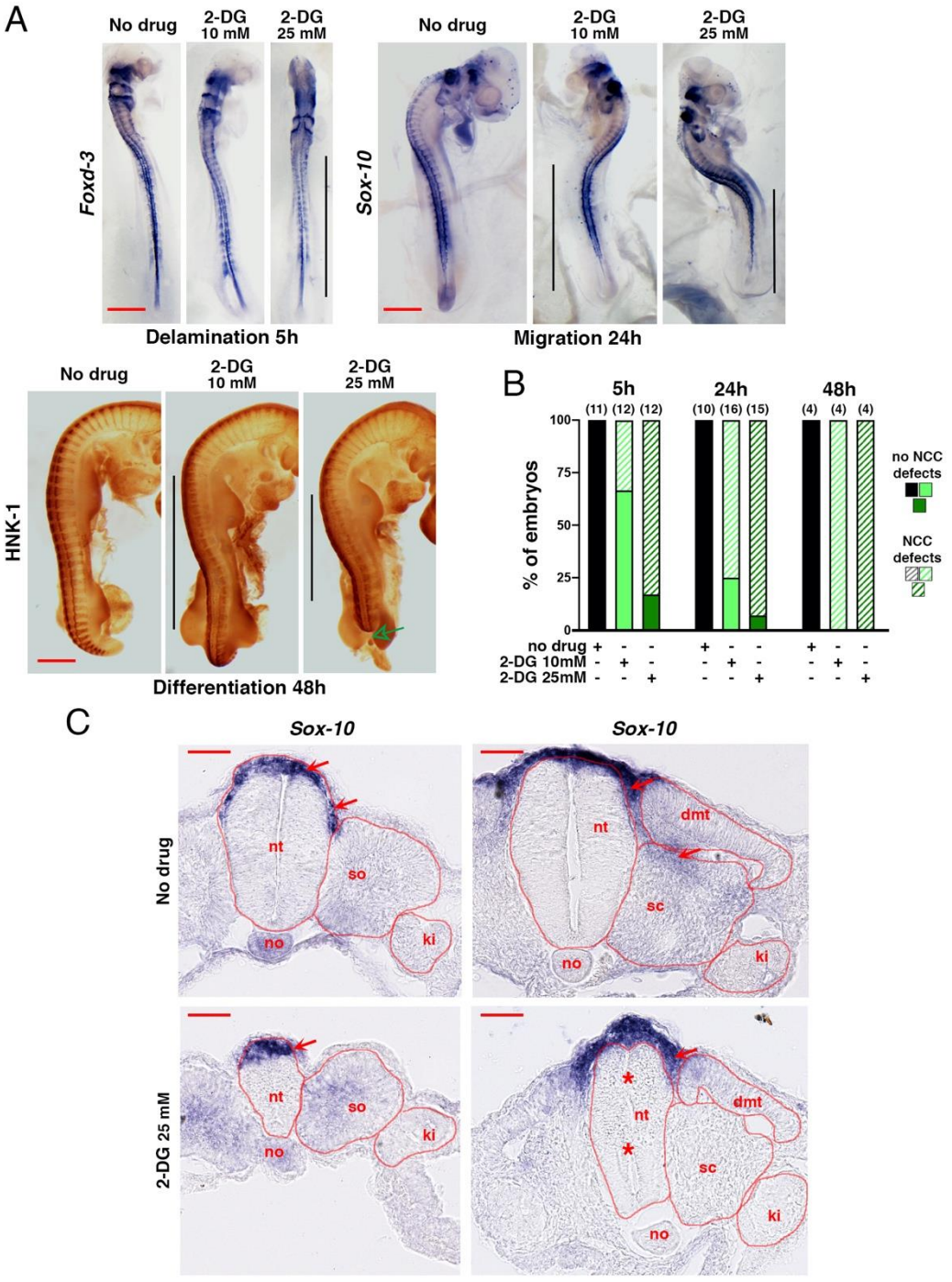

Supplementary Figure 2 : Nekooie-Marnany et al.

Fig. S2, related to Fig.1.

(A) Whole mount views of ISH with probes for *Foxd-3*, *Sox-10* mRNAs, and of immunolabeling for HNK-1, showing the whole embryo 5 h, 24h and 48 h after 2-DG or vehicle injection. Vertical bars delineate the axial levels where NCC development is defective. The green arrow points to the truncated tail of the embryo 48 h after treatment with 2-DG at 25 mM. Note that the cranial structures and NCCs are not affected by caudal injection of 2-DG even at high concentrations. The corresponding views of the embryos at the trunk level are shown in Fig.1D. (B) Proportion of embryos with normal morphology (filled bars) or presenting with NCC defects (hatched bars), 5 h, 24 h and 48 h after injection with vehicle (black columns) or 2-DG at 10 mM (light green) and 25 mM (dark green). (C) Cross-sections through the caudal (left), and mid (center), trunk of embryos 24 h after injection with the vehicle (upper panels) or 2-DG at 25 mM (lower panels) and processed for whole mount ISH for *Sox-10*. Arrows point at NCCs. The NT, somite, sclerotome, dermamyotome and kidney primordium have been circled to illustrate the reduced size and abnormal morphology of the axial and paraxial structures (NT and somites) compared with more lateral structure such as the kidney primordium in the presence of 2-DG. Asterisks indicate abnormalities in the NT lumen. Data were collected from at least three independent experiments. (n) indicate the number of embryo analyzed. Images in A and C are representative of at least three independent experiments. Scale bars in A, 500 µm; and C, 100 µm. ec, ectoderm; dmt, dermamyotome; ki, kidney promordium; no, notochord; nt, neural tube; sc, sclerotome; so, somite.

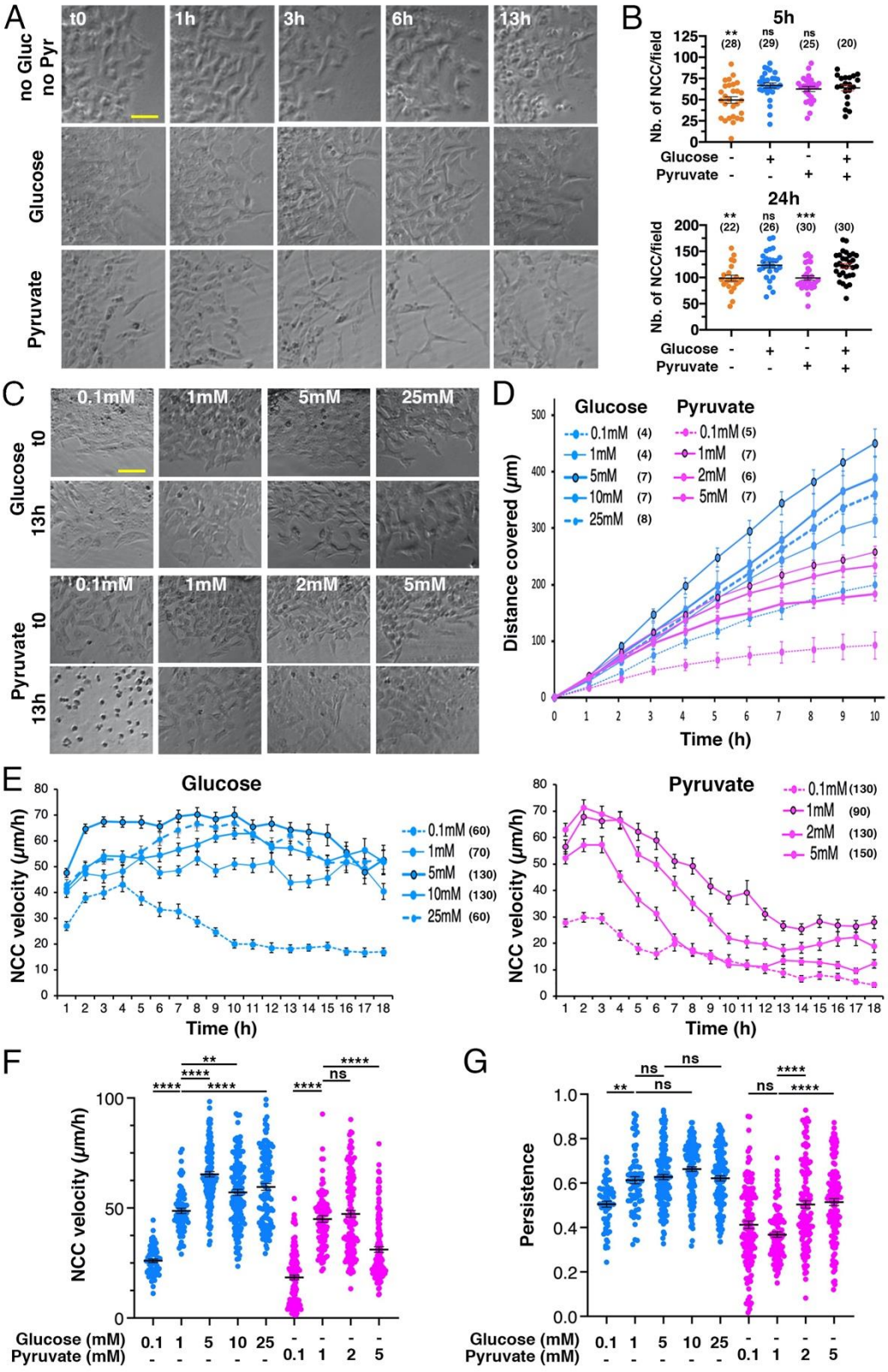

Supplementary Figure 3: Nekooie-Marnany et al.

Fig. S3, related to Fig.1.

(A) Morphological aspect of NCCs at the migratory front at different time points of cultures in medium without glucose and pyruvate (no Gluc-no Pyr, top) or in the presence of 5 mM glucose or 1 mM pyruvate. Images were extracted from video-microscopic recordings performed as follows: trunk NT explanted in 8-well chambered glass coverslips coated with fibronectin and NCCs were allowed to initiate outward migration for about 2-4 h before video-microscopy started, defined as t0. (B) Scatter plot with mean ± s.e.m of the cell density in NCC outgrowth at 5 and 24 h in conditions as in A, analyzed using one-way ANOVA followed by Dunnett's multiple comparison test relative to the glucose and pyruvate condition. (C) Morphological aspect of NCCs at the migratory front at t0 and after 13 h in glucose or in pyruvate at different concentrations. Images were extracted from video-microscopic recordings as in A. (D) Curves of mean distance covered by the migratory front of the NCC population in medium with different glucose or pyruvate concentrations, analyzed throughout 10-h recording using a custom GUI written in Matlab. (E) Graphs of velocity of individual NCC over time in medium containing glucose or pyruvate at various concentrations throughout 18-h video-microscopy recordings, analyzed using Metamorph software. Values are mean ± s.e.m. and (n) indicate the total number of NCCs analyzed in several NT explants with 20 NCCs tracked at the periphery of the outgrowth on each side of NT. (F-G) Scatter plots with mean ± s.e.m of the velocity (F) and persistence (G) of individual NCC throughout the 18-h video microscopy recording, analyzed using one-way ANOVA followed by Dunnett's multiple comparison test. Data were collected from at least three independent experiments. Images in A and C are representative of at least three independent experiments. (n) indicate the number of trunk NT explants analyzed. In F and G, n are the same than those in E. ** $P<0.01$, *** $P<0.001$, **** $P<0.0001$; ns, not statistically significant, $P>0.05$. Scale bar in A and C = 50 µm.

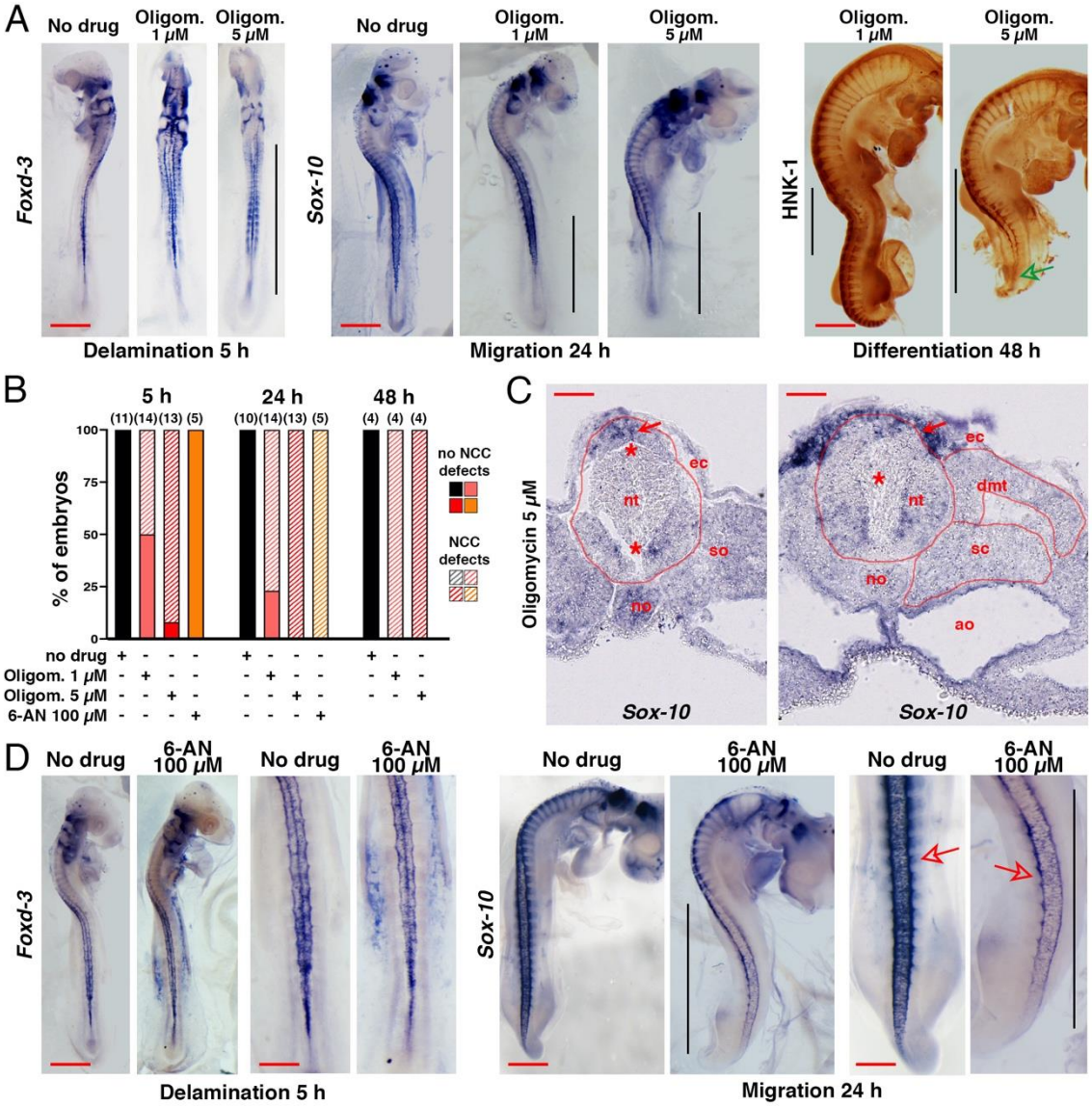

Supplementary Figure 4: Nekooie-Marnany et al.

Fig. S4, related to Fig. 3.

(A) Whole mount views of ISH with probes for *Foxd-3*, *Sox-10* mRNAs, and of immunolabeling for HNK-1, showing the whole embryo 5 h, 24h and 48 h after oligomycin or vehicle injection. Vertical bars delineate the axial levels where NCC development is defective. The green arrow points to the truncated caudal half of the embryo 48 h after treatment with oligomycin at 5 µM. Note that as for 2-DG, the cranial structures and NCCs are not affected by caudal injection of oligomycin even at high concentrations. The corresponding views of the embryos at the trunk level are shown in Fig.3B. (B) Proportion of embryos with normal morphology (filled bars) or presenting with NCC defects (hatched bars), 5 h, 24 h and 48 h after injection with vehicle (black columns), oligomycin at 1 µM (light red columns) and 5 µM (dark red columns), or 6-AN at 100 µM (orange columns). (C) Cross-sections through the caudal (left), and mid (right) trunk of embryos 24 h after injection with oligomycin at 5 µM and processed for whole mount ISH for *Sox-10*. Arrows point at NCCs. The NT, somite, sclerotome, and dermamyotome have been circled to illustrate the severe morphological alterations of the NT and somites. Asterisks indicate abnormalities in the NT lumen. (D) Whole mount views of ISH with probes for *Foxd-3*, *Sox-10* mRNAs, and of immunolabeling for HNK-1, showing the whole embryo (left panels for each probe) and detail of the trunk (right panels for each probe), 5 h, 24h and 48 h after 6-AN or vehicle injection. Vertical bars delineate the axial levels where NCC development is defective. The arrows point to migrating NCCs. Data were collected from at least three independent experiments. (n) indicate the number of embryo analyzed. Images in A and C are representative of at least three independent experiments. Scale bars in A, 500 µm; in C, 100 µm; and in D, 500 µm for the overall views of embryos and 100 µm for the closer views of the trunk. ao, aorta; ec, ectoderm; dmt, dermamyotome; no, notochord; nt, neural tube; sc, sclerotome; so, somite.

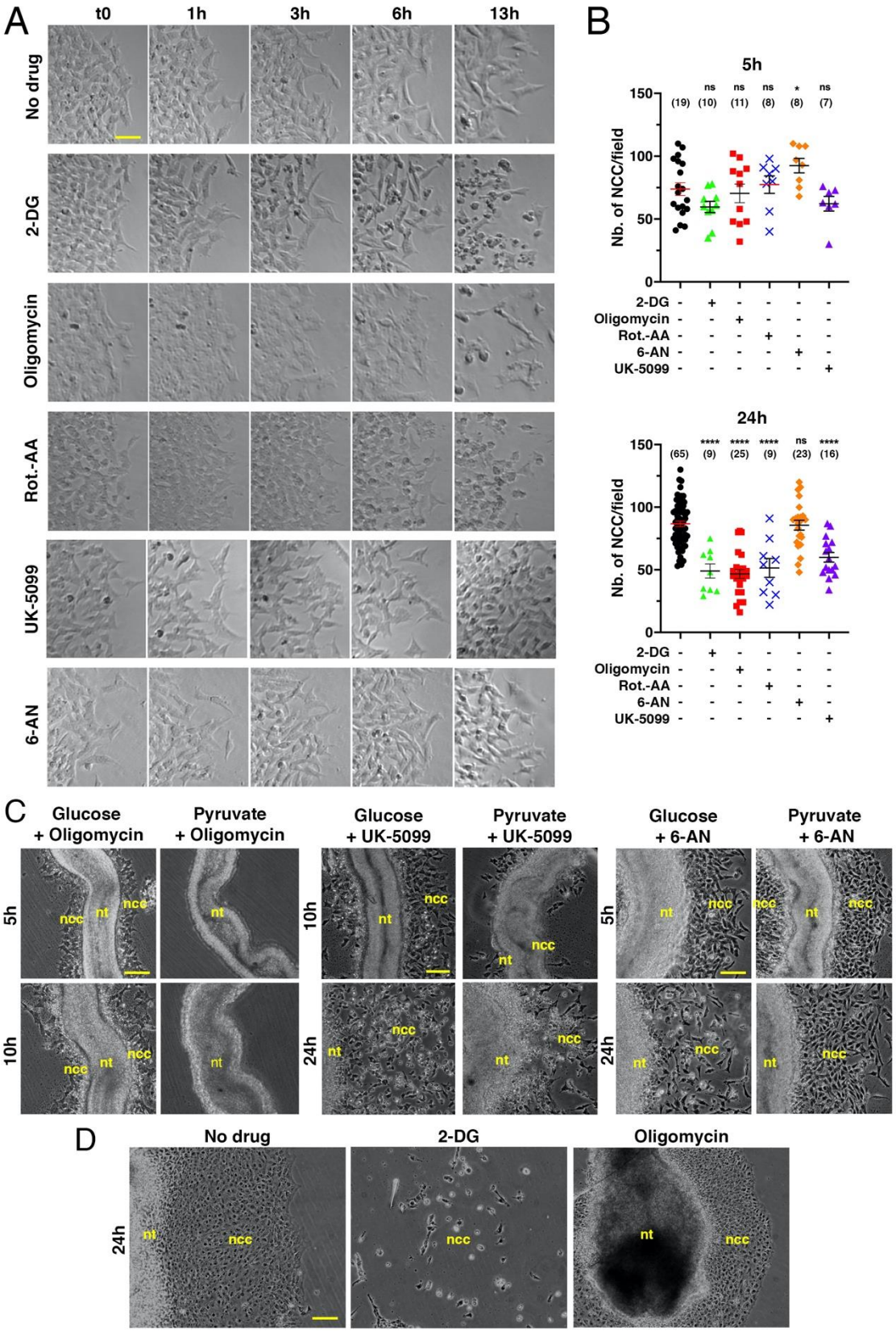

Supplementary Figure 5: Nekooie-Marnany et al.

Fig. S5, related to Fig. 3.

(A) Morphological aspect of NCCs at the migratory front at different time points of cultures in glucose and pyruvate medium with metabolic inhibitors. Images were extracted from video-microscopic recordings performed as follows: trunk NT explanted in 8-well chambered glass coverslips coated with fibronectin and NCC were allowed to initiate outward migration for about 2-4 h before video-microscopy started, defined as t0. (B) Scatter plot with mean ± s.e.m of the cell density in NCC outgrowth at 5 and 24 h in conditions as in A, analyzed using one-way ANOVA followed by Dunnett's multiple comparison test relative to the glucose and pyruvate condition. (C) Overall aspect of trunk NT explants at different times in culture in medium with glucose alone or pyruvate alone in the presence of 1 µM oligomycin, 100 µM UK-5099, or 100 µM 6-AN. (D) Overall aspect of cranial NT explants at 24 h in medium with glucose and pyruvate (no drug) and in the presence of 1 mM 2-DG or 1 µM oligomycin. Data were collected from at least three independent experiments. Images in A, C and D are representative of at least three independent experiments. (n) indicate the number of trunk NT explants analyzed. ** $P<0.01$, *** $P<0.001$, **** $P<0.0001$; ns, not statistically significant, $P>0.05$. Scale bar in A, 50 µm; and in C, D, 100 µm. nt, neural tube.

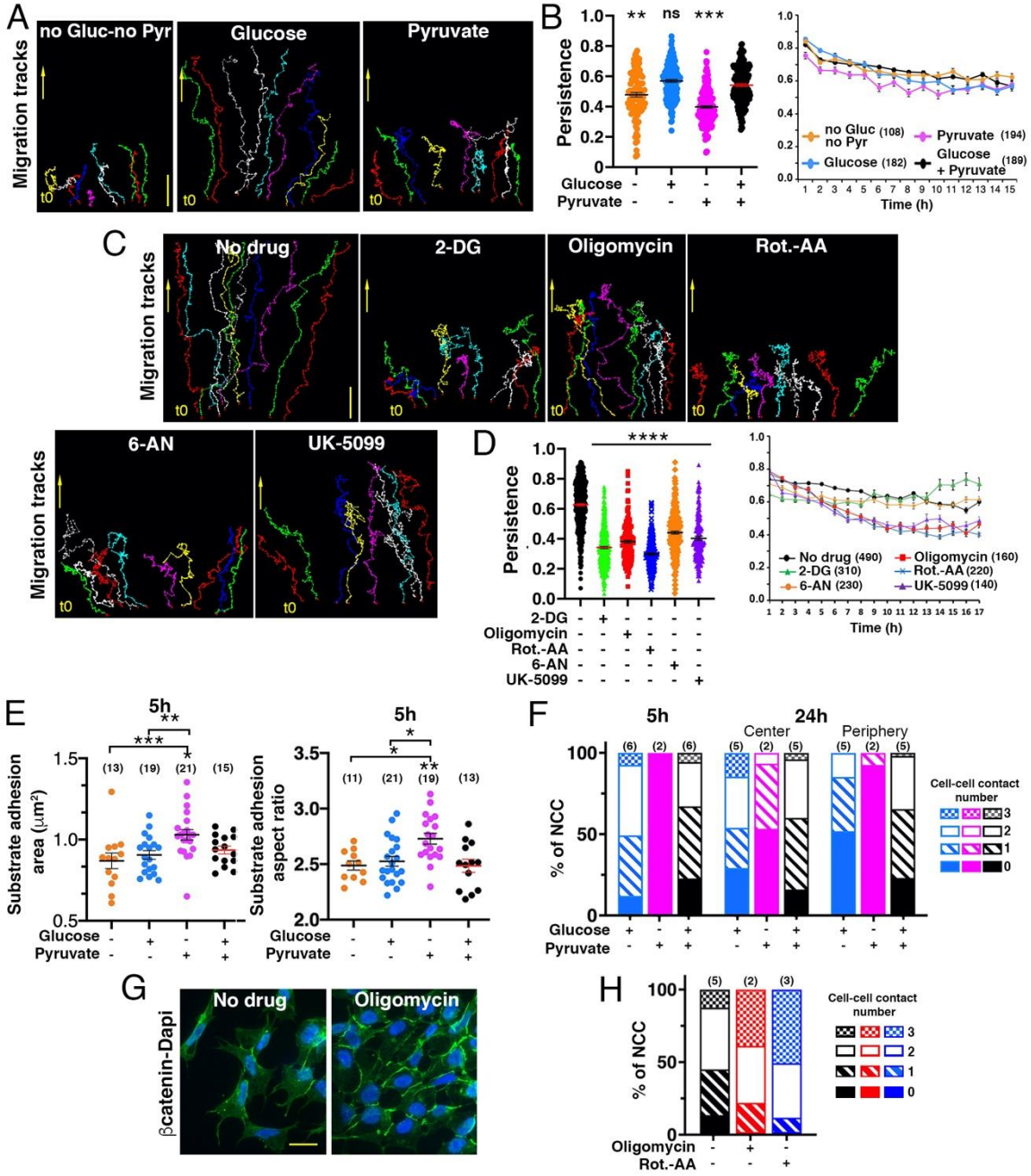

Supplementary Figure 6: Nekooie-Marnany et al.

Fig. S6, related to Fig. 5.

(A-D) Migration properties of NCCs in various nutrients conditions and in the presence of metabolic inhibitors. (A, C) Migration tracks of several NCCs from a representative NT explant in indicated nutrient conditions (A), or in glucose and pyruvate medium in the presence of metabolic inhibitors (C). NCCs were allowed to initiate outward migration from trunk NT explants cultured in 8-well Chambered Coverglass for about 2-4 h before video-microscopy started, defined as t0. Drugs were added immediately before recording. The initial position of the cells is indicated at t0 and the direction of migration is given by the yellow arrow. (B, D) Scatter plots with mean ± s.e.m of the persistence (left) and curves of the persistence over time (right) of individual NCC expressed as with mean ± s.e.m throughout the video-microscopy recording in indicated nutrient conditions (B) or in glucose and pyruvate medium with metabolic inhibitors (D). (n) indicates the total number of NCCs analyzed in several NT explants, with for each NT explant 20 NCCs analyzed at the periphery of the outgrowth. (E) Scatter plot with mean ± s.e.m of the area of substrate adhesions (left) and their aspect ratio (right) in the indicated nutrient conditions. (F-H) Cell-cell adhesion properties of NCCs in defined nutrient conditions and with metabolic inhibitors. (F) Number of cell-cell contacts formed by migrating NCCs formed with their neighbors at 5 h, and at the center or the periphery of the outgrowth at 24 h. Data were obtained from images of trunk immunostained for β-catenin and are expressed as the proportions of NCC with 0-3 contacts/cell. (G) Immunolabeling for β-catenin (green) and nuclei visualization using Dapi (blue) in NCCs cultured for 5 h in the presence of oligomycin compared with no drug condition. (H) Number of cell-cell contacts in migrating NCCs cultured in glucose and pyruvate medium with metabolic inhibitors. Data were obtained and are expressed as in F. (I) Cell-substratum adhesion properties of NCCs in defined nutrient conditions. Immunolabeling for paxillin (green), filamentous actin (red), and nuclei visualization using Dapi (blue) in NCCs cultured for 5 h on stiff (6.3 kPa) and soft (1.2 kPa) PAA-gels coated with fibronectin in indicated nutrient conditions. Data were collected from at least three independent experiments. Images in A, C, G and I are from representative experiments. Scatter plots were analyzed using one-way ANOVA followed by Dunnett's multiple comparison test relative to the glucose and pyruvate condition (B, D) or to the medium with glucose alone (E). *P<0.05, **P<0.01, ***P<0.001,****P<0.0001; ns, not significant, P>0.05. Bars in A and C = 100 µm, G = 20 µm and I = 25 µm. Scale bar in A, 100 µm; and in G, I, 25 µm.

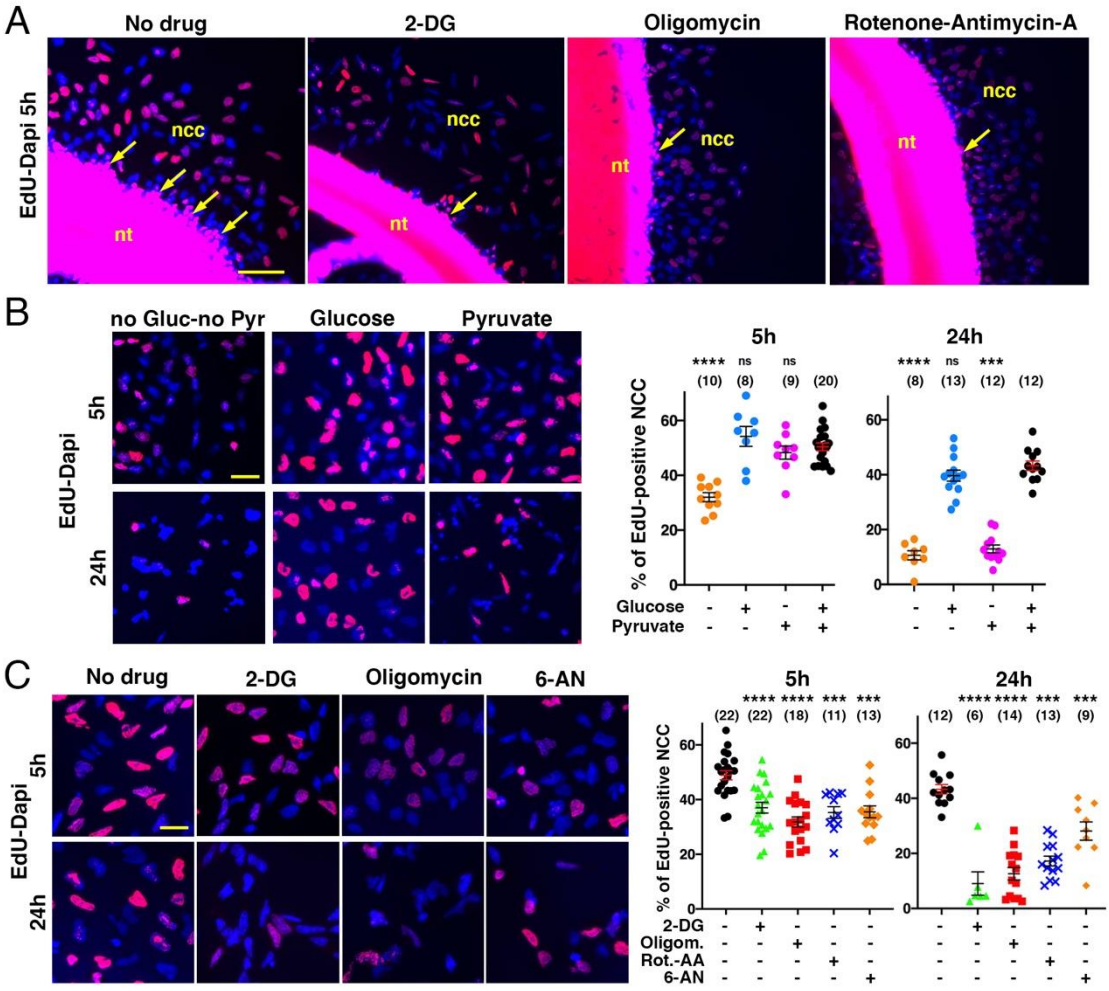

Supplementary Figure 7: Nekooie-Marnany et al.

Fig. S7.

(A) Images of EdU incorporation (pink) and visualization of nuclei using Dapi (blue) in NT explants cultured for 5 h in glucose and pyruvate medium with metabolic inhibitors. Arrows point on NCCs delaminating out of the NT, which are EdU+, as some of the migrating NCCs. (B, C) Images of EdU incorporation (pink) and visualization of nuclei using Dapi (blue) (left) and scatter plot with mean ± s.e.m of the proportion of EdU-positive NCCs (right) in NT explants cultured for 5 h or 24 h in indicated nutrient condition (B) and in glucose and pyruvate medium with inhibitors (C). (n) indicate the number of NT explants analyzed. Scatter plots were analyzed using one-way ANOVA followed by Dunnett's multiple comparison test relative to the condition without the drug. Data were collected from at least three independent experiments. Images are from representative experiments. *** $P<0.001$, **** $P<0.0001$; ns, not statistically significant, $P>0.05$. Scale bar in A, 50 µm; and in B, C, 20 µm. nt, neural tube.

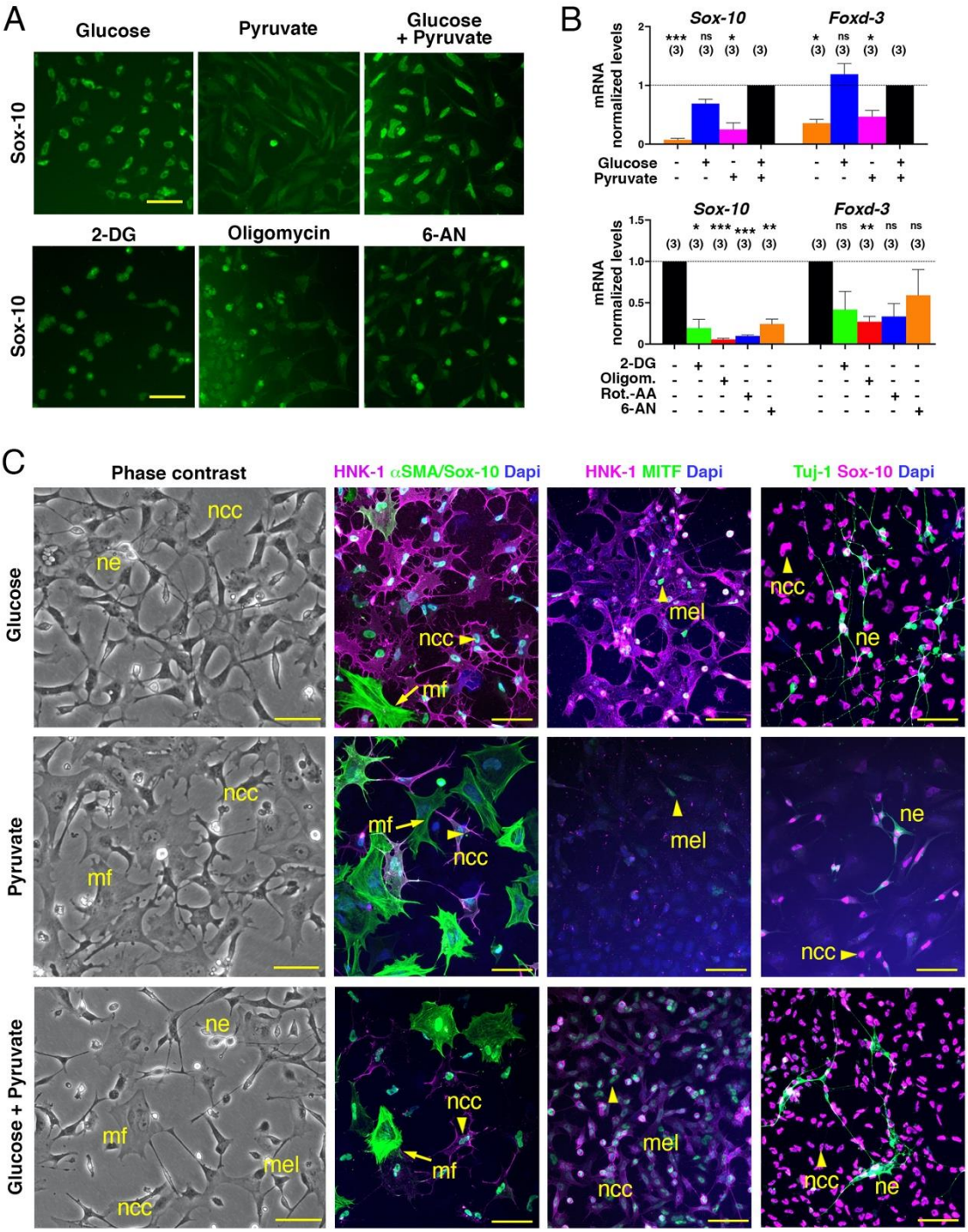

Supplementary Figure 8: Nekooie-Marnany et al.

Fig. S8, related to Fig. 6.

(A) Immunostaining for Sox-10 in NCCs from trunk NT explants cultured for 24 h in indicated nutrient conditions (top) and with metabolic inhibitors (bottom). (B) Normalized levels of *Sox-10* and *Foxd-3* mRNA measured by qRT-PCR from NT explants cultured for 24 h in indicated nutrient conditions (top), and in glucose and pyruvate medium with metabolic inhibitors (bottom), with three. Values are mean ± s.e.m of triplicates per medium condition and gene analyzed using unpaired t-test two-tailed. (n) indicate the number of experiments. * $P<0.05$, ** $P<0.01$, *** $P<0.001$; ns, not significant, $P>0.05$. (C) Phase contrast and immunofluorescence images for pluripotency and differentiation markers, with nuclei labelled with Dapi (blue) showing the morphology and heterogeneity of the NCC population after 3 days in culture in medium containing glucose (top), pyruvate (middle) or both nutrients (bottom). Nuclear Sox-10 and HNK-1 mark undifferentiated NCC progenitors (arrowhead), α-SMA myofibroblasts (mf, arrows; left panels), nuclear MITF melanoblasts (mel, arrows, also negative for HNK1; middle panels), and Tuj-1 neurons (ne, in green right panels) with elongated neurites. Data were collected from at least three independent experiments. Images in A and C are from representative experiments. Scale Bars, 50 µm.